Evaluation of Quenching Factor in Ce^{3+}-Doped Y_2SiO_5 Nanoscintillators for α and γ Radiation Detection

Billel Zahra[(1)*], Lakhdar Guerbous[(2)], Mohammed Salah Eddine Hamroun[(3)], Hamza Mekki[(1)]
[(1)] Nuclear Detection & Instrumentation Department, Nuclear Research Center of Birine, B.P: 180 Ain Oussera, Djelfa, Algeria
[(2)] Department of Radiological and Atomic Physics, Nuclear Research Center of Algiers, 02, Bd Frantz Fanon, B.P. 399, Algiers, 16000, Algeria
[(3)] Centre de Recherche Scientifique et Technique en Analyses Physico-Chimiques, BP 384, Zone Industrielle, Bou-Ismail CP 42004, Tipaza, Algeria
*Corresponding author b.zahra@crnb.dz

Abstract: The quenching factor (QF), defined as the α/γ light output ratio, is a key parameter for evaluating the radiation discrimination performance of scintillators. In this study, five sample detectors were fabricated using $Y_2SiO_5:Ce^{3+}$ nanophosphor powders synthesized at different annealing temperatures of the xerogels, specifically 900 °C, 950 °C, 1000 °C, 1050 °C, and 1250 °C. The detectors were tested under excitation by α-particles (from ^{241}Am, 5.48 MeV) and γ-rays (from ^{137}Cs, 662 keV). The QF was determined from the pulse-height spectra by comparing the α- and γ-induced peak positions and normalizing the measured light output to the corresponding deposited energies and electronic gains. A QF value of 0.46 was obtained for the YSO_1250 sample, indicating a significant reduction in quenching at higher annealing temperatures. Conversely, samples treated at lower temperatures exhibited stronger quenching, with QF values as low as 0.17. This trend is attributed to improved crystallinity and reduced defect density at elevated temperatures, which enhance scintillation efficiency for highly ionizing α-particles. These findings demonstrate that annealing temperature serves as an effective tuning parameter for optimizing the QF and, consequently, the scintillator's suitability for either α/γ discrimination or α-sensitivity, depending on the application.

Keywords: Scintillator, Quenching factor; YSO: Ce^{3+}; α/γ ratio; Radiation detection; Nanophosphors.

1. INTRODUCTION

The accurate detection and discrimination of ionizing radiation including α-particles, γ-rays, and β-particles are critical in a wide range of applications such as nuclear security, environmental monitoring, and fundamental physics experiments like dark matter searches and rare-event detection [1–6]. Among the various detection techniques, scintillation detectors are widely used due to their high sensitivity and versatility in detecting different radiation types. These detectors operate by converting radiation energy into measurable light pulses. However, their performance is strongly affected by the quenching effect, wherein heavily ionizing particles such as α-particles produce significantly less scintillation light per unit energy deposited compared to lightly ionizing particles like γ-rays or electrons.

A key metric for characterizing this behavior is the quenching factor, defined as the ratio of the light yield from α-particles to that from γ-rays at the same energy deposition. Typically, a QF less than 1 indicates light output suppression for α-particles due to high ionization densities along their tracks, which promote non-radiative recombination in accordance with Birks' law [7,8]. Interestingly, materials such as ZnSe(Te) have exhibited anomalous behavior with QF values greater than 1, defying conventional models and presenting unique opportunities for particle discrimination [9].

The QF varies considerably across scintillator classes, reflecting differences in electronic structure, defect chemistry, and energy transfer mechanisms. Oxide scintillators such as BGO, CWO, and GSO:Ce generally display low QF values in the range of ~0.20–0.21, which limits their suitability for α-particle detection despite offering good energy resolution for γ-rays [10]. This low QF in oxides is primarily attributed to lattice defects and the high ionization density of α-tracks, which promote non-radiative recombination. In contrast, alkali halide scintillators like CsI(Tl) and NaI(Tl) exhibit moderate QF values (0.45–0.67), associated with more efficient energy transfer to luminescent centers [10]. Semiconductor materials such as ZnSe(Te) demonstrate anomalous QF values exceeding 1, often attributed to defect-mediated luminescence, although challenges remain regarding

scalability and reproducibility [3]. Liquid noble gases like liquid argon (LAr) exhibit energy-dependent QF behavior, making them suitable for background suppression in precision experiments [7]. These examples illustrate that QF is a complex function of material properties, defect structure, and excitation conditions.

Within the oxide scintillator family, orthosilicates have emerged as particularly attractive candidates due to their high density, good chemical stability, and excellent light yield when appropriately doped. Among these, cerium-doped yttrium orthosilicate ($Y_2SiO_5:Ce^{3+}$, or YSO:Ce) is of particular interest because Ce^{3+} ions provide fast 5d→4f radiative transitions with nanosecond-scale decay times, making it suitable for high-count-rate applications.

In nanostructured scintillators, the high surface-to-volume ratio and grain-boundary density make the material particularly sensitive to processing conditions. Annealing temperature, in particular, plays a decisive role in determining crystallinity, grain size, and defect density, all of which directly influence energy transfer efficiency and the probability of non-radiative recombination. Higher annealing temperatures promote grain growth and reduce structural defects that act as quenching centers [13]. These microstructural changes are expected to differentially affect the scintillation response to α-particles versus γ-rays, given the higher susceptibility of dense ionization tracks to quenching by structural imperfections.

The QF is influenced by various external and internal factors. These include the material's composition and defect structure, for example, ZnSe exhibits QF inversion behavior following annealing, due to the disruption of {Zn_i–V_Zn} defect complexes [3]. Temperature also plays a critical role; alkali halides such as CsI(Tl) display strong QF temperature dependence, with increases up to 35% observed at –20 °C, a behavior not commonly observed in oxide-based scintillators [10]. The signal integration time further affects QF measurements: slow scintillation components, especially in CsI(Tl), lead to increased QF when longer integration windows are used [10]. Finally, particle quenching, such as energy loss in non-scintillating regions (e.g., in plastic scintillator microspheres), may reduce the overall detection efficiency, especially in the case of low-energy β-emitters [8].

Despite notable progress in understanding quenching factor (QF) behavior in scintillators, several important research gaps remain. In particular, the influence of thermal treatment parameters, such as annealing temperature, on the QF in nanostructured scintillator materials remains insufficiently explored. While numerous studies have focused on material composition and doping [11,12], systematic investigations linking annealing conditions to QF behavior are still limited.

In this work, five sample detectors were fabricated using $Y_2SiO_5:Ce^{3+}$ nanophosphor powders synthesized at different annealing temperatures of the xerogels, specifically 900 °C, 950 °C, 1000 °C, 1050 °C, and 1250 °C. The aim is to contribute to bridging the current knowledge gap by evaluating the effect of annealing temperature on the QF of Ce^{3+}-doped Y_2SiO_5 nanophosphor-based detectors. Through this study, we aim to demonstrate that annealing temperature serves as an effective tuning parameter for optimizing the QF and, consequently, enhancing the scintillator's suitability for either α/γ discrimination or improved α-particle sensitivity, depending on the specific application.

2. EXPERIMENTAL

In our previous study [13], we synthesized Cerium (Ce^{3+})-doped Y_2SiO_5 (YSO: Ce^{3+}) type oxyorthosilicate powders using the sol–gel method. Following synthesis, we conducted an extensive investigation into the effect of annealing temperature on the structural and photoluminescent properties of the YSO: Ce^{3+} samples. Utilizing these synthesized powders, we fabricated sample radiation detectors with the primary goal of studying the effect of annealing temperature on the quenching factor for achieving highly efficient radiation detectors. The fabrication process for the sample detectors follows the same methodology described in our previous work [14]. Figure 1a illustrates some powder samples with different annealing temperature and Figure 1b present a photograph of designed sample detector annealed at 1000 °C. All sample detectors in this study underwent the same fabrication procedure and adhered to identical dimensions of 20 × 15 × 1 mm^3. For simplification, the prepared sample detectors were named: YSO_900, YSO_950, YSO_1000, YSO_1050 and YSO_1250, according to the annealing temperature used during the synthesis process.

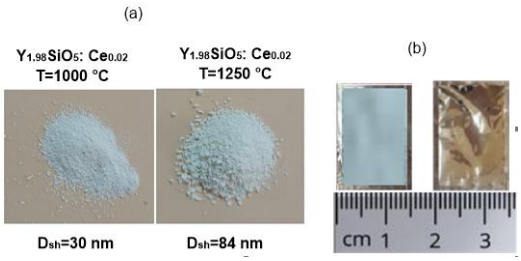


Fig. 1 (a) YSO: Ce^{3+} sample powders annealed at 1000 °C and 1250 °C with corresponding crystallite sizes (D_{sh}), (b) Photograph of the prepared sample detector YSO_1000

Scintillation pulse-height spectra were acquired at room temperature using 662 keV γ-rays from a ^{137}Cs source (24.8 kBq) and 5.48 MeV α-particles from an ^{241}Am source (48.2 kBq). The sample detectors were coupled to a GDB-4FF photomultiplier tube serving as the photodetector. The electronic chain consisted of an ORTEC 465 high-voltage power supply, an ORTEC 113 preamplifier, an ORTEC 672 pulse-shaping amplifier, an ORTEC 927-ASPEC multichannel analyzer, and a PC equipped with Maestro software. Further details regarding the experimental setup can be found in a previous report [11]. Because the scintillation response under α-particle excitation increased considerably with rising annealing temperature, the amplifier gain for the α measurements was adjusted for the YSO_1050 and YSO_1250 detectors to maintain the corresponding pulse-height peaks within the optimum dynamic range of the multichannel analyzer and to avoid signal saturation. The gain correction was explicitly included in Eq. (1). The linearity of the pulse-processing chain was verified over the gain range used in the measurements (100–300), and good linearity was observed for the peak-position determination.

The quenching factor, often referred to as the relative α/γ light output ratio, is a key parameter in the characterization of scintillators, particularly in their ability to respond differently to various types of radiation. It essentially measures how efficiently the scintillator converts the energy of charged particles (such as alpha particles) into scintillation light compared to gamma rays. When alpha particles interact with scintillator detector, a considerable amount of energy is converted by other ways, instead of scintillation light. The quenching factor is mathematically defined as [15]:

$$QF = \frac{P_{\alpha/E_\alpha}}{P_{\gamma/E_\gamma}} \cdot \frac{G_\gamma}{G_\alpha} \quad (1)$$

Where:

P_α: is the peak position of the α particles, E_α: is the energy of the alpha particles, P_γ: is the peak position of the gamma rays and E_γ: is the energy of the gamma rays, with G_α and G_γ as their respective gains.

3. RESULTS AND DISCUSSION

The YSO:Ce^{3+} sample detectors were irradiated with 5.48 MeV α-particles from a ^{241}Am source and 662 keV γ-rays from a ^{137}Cs source. The corresponding results are presented in Figure 2, where the recorded pulse-height spectra were analyzed using Gaussian fitting to extract the peak positions associated with α (P_α) and γ (P_γ) interactions for each sample. Based on Equation (1), the corresponding QF were then calculated. These values, along with the experimental parameters used during the measurements, are summarized in Table 1.

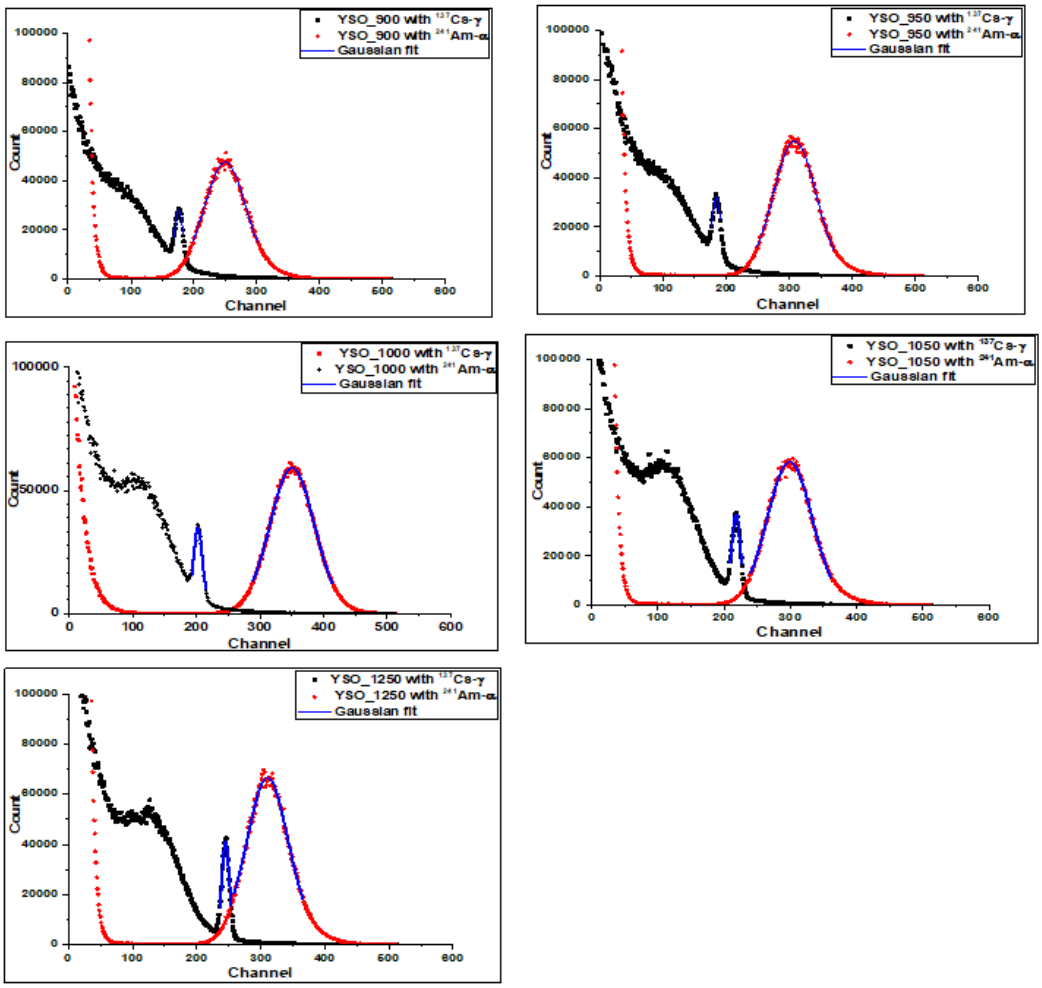


Fig. 2 Pulse height spectra of: ^{137}Cs-γ and ^{241}Am-α fitted by Gaussian function measured by studied sample detectors

Table 1 QF as function of annealing temperature of YSO: Ce^{3+} nanoscintillator

Sample detectors	Peak position P_α	Peak position P_γ	Gain G_α	Gain G_γ	QF
YSO_900	250±0.17	176±0.16	300	300	0.17±0.002
YSO_950	309±0.14	185±0.11	300	300	0.19±0.002
YSO_1000	350±0.10	202±0.09	300	300	0.21±0.001
YSO_1050	299±0.14	218±0.09	150	300	0.33±0.002
YSO_1250	310±0.17	245±0.06	100	300	0.46±0.003

The quenching factor (QF) of Ce^{3+}-doped Y_2SiO_5 nanoscintillators exhibits a strong dependence on annealing temperature, driven by the interplay between radiation–matter interaction physics and the evolving microstructure of the material. At lower annealing temperatures (900–1000 °C), QF values remain low (0.17–0.21), reflecting substantial light suppression in response to α-particles. This behavior is fundamentally governed by the high linear energy transfer (LET) of α-particles, which produce dense ionization tracks with elevated excitation densities. According to Birks' law, the light yield per unit energy deposited decreases with increasing ionization density due to enhanced probability of non-radiative recombination and saturation of luminescence centers [7,8]. This quenching effect is further exacerbated at lower annealing temperatures by the poor crystallinity, small grain size, and high concentration of structural defects and trap states, which act as non-radiative decay channels that disproportionately affect the already energy-dense α-tracks. In contrast, γ-rays interact via lower-LET mechanisms, such as compton scattering, producing sparsely ionizing electrons that are less susceptible to

quenching, thus resulting in higher light yield. As the annealing temperature exceeds 1000 °C, QF increases sharply, reaching 0.33 at 1050 °C and 0.46 at 1250 °C signaling a reduction in quenching for α-particles. This enhancement is consistent with the improved crystallinity and grain growth reported in the XRD and SEM analyses of the corresponding samples in [13]. These structural changes may favor radiative recombination and contribute to the observed increase in light yield, particularly under heavily ionizing radiation. Moreover, the observed behavior may also stem from a concomitant reduction in defect-related trapping, which would otherwise act as non-radiative recombination centers. Figure 3 illustrates the correlation between QF values and crystallite sizes of the elaborated YSO:Ce powders as a function of annealing temperature, further supporting the role of structural evolution in tuning scintillation performance. These results underline how annealing temperature not only controls the structural integrity of the scintillator but also tunes its α/γ response through mechanisms rooted in both material quality and ionization physics, providing a practical pathway to tailor QF for specific radiation detection requirements.

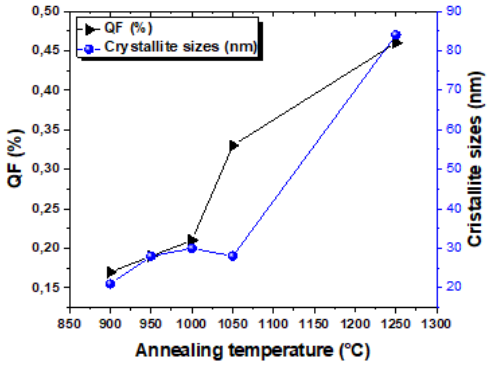


Fig. 3 Evolution of the quenching factor and crystallite size of Ce^{3+}-doped Y_2SiO_5 nanophosphor powders as a function of annealing temperature.

For comparison with other scintillation materials, the QF values obtained for the present YSO nanoscintillators span the range from 0.17 to 0.46. The QF obtained for YSO_900 (0.17) is slightly lower than the values reported for several oxide scintillators such as BGO, CWO, and GSO, which are typically around 0.20–0.21 [10]. In contrast, the QF of YSO_1250 (0.46) approaches the lower part of the range reported for alkali-halide scintillators such as CsI(Tl) and NaI(Tl), for which values of approximately 0.45–0.67 have been reported [10]. Thus, although the QF values of the present YSO^{3+} detectors remain below unity, the substantial increase from 0.17 to 0.46 demonstrates that thermal treatment can significantly modify the relative scintillation response to α-particles.

4. CONCLUSION

In this study, the quenching factor of Ce^{3+}-doped Y_2SiO_5 nanoscintillators was systematically investigated as a function of annealing temperature. Five sample detectors were fabricated from nanophosphor powders annealed between 900 °C and 1250 °C, and their scintillation responses to both α-particles and γ-rays were characterized. The results demonstrate a clear dependence of QF on the thermal treatment conditions. At lower annealing temperatures (900–1000 °C), QF values remained relatively low (0.17–0.21), indicating strong quenching of α-particles, primarily due to poor crystallinity, small grain size, and high defect concentrations. These structural imperfections favor non-radiative recombination and thus suppress the scintillation yield under heavy ionizing radiation. As the annealing temperature increased beyond 1000 °C, QF values improved significantly, reaching 0.33 at 1050 °C and 0.46 at 1250 °C, suggesting a reduced quenching effect resulting from enhanced crystallinity, grain growth, and fewer trap states.

These findings demonstrate that annealing temperature is an effective parameter for tuning the relative α/γ scintillation response of $Y_2SiO_5:Ce^{3+}$ nanoscintillators. The lower QF values obtained at 900–1000 °C indicate stronger suppression of the scintillation response to highly ionizing α-particles, resulting in a larger difference between the α- and γ-induced light outputs. Such a response may be advantageous in applications where differences in light output are exploited for radiation-type discrimination. In contrast, the higher QF values obtained at 1050–1250 °C indicate reduced α-particle quenching and therefore a more efficient conversion of deposited α-particle energy into scintillation light, which may be preferable for applications requiring enhanced α-particle detection sensitivity.

This study provides valuable insight into the relationship between synthesis conditions, material structure, and radiation response, contributing to the development of optimized nanoscintillator-based detectors for mixed-radiation environments. As a future

perspective, the QF could be further tailored by investigating the influence of Ce^{3+} doping concentration on the scintillation behavior under different types of radiation.

References

[1] C. Coppi, C. Ciemniak, F. von Feilitzsch, A. Gütlein, H. Hagn, C. Isaila, J. Jochum, M. Kimmerle, J.-C. Lanfranchi, S. Pfister, W. Potzel, W. Rau, S. Roth, K. Rottler, C. Sailer, S. Scholl, I. Usherov, W. Westphal, Characterization of the CRESST detectors by neutron induced nuclear recoils, EAS Publ. Ser. 36 (2009) 315–317. https://doi.org/10.1051/eas/0936045.

[2] H. Chagani, P. Majewski, E.J. Daw, V.A. Kudryavtsev, N.J.C. Spooner, Measurement of the scintillation efficiency of Na recoils in NaI(Tl) down to 10 kev nuclear recoil energy relevant to dark matter searches, in: Proc. 6th Int. Work. Identif. Dark Matter, IDM 2006, WORLD SCIENTIFIC, 2007: pp. 262–267. https://doi.org/10.1142/9789812770288_0035.

[3] E. Aprile, L. Baudis, B. Choi, K.L. Giboni, K. Lim, A. Manalaysay, M.E. Monzani, G. Plante, R. Santorelli, M. Yamashita, New measurement of the relative scintillation efficiency of xenon nuclear recoils below 10 keV, Phys. Rev. C 79 (2009) 45807. https://doi.org/10.1103/PhysRevC.79.045807.

[4] B. Lenardo, J. Xu, S. Pereverzev, O.A. Akindele, D. Naim, J. Kingston, A. Bernstein, K. Kazkaz, M. Tripathi, C. Awe, Measurement of the ionization yield from nuclear recoils in liquid xenon between 0.3--6 keV with single-ionization-electron sensitivity, ArXiv Prepr. ArXiv1908.00518 (2019).

[5] D.S. Akerib, S. Alsum, H.M. Araújo, X. Bai, J. Balajthy, J. Bang, A. Baxter, E.P. Bernard, A. Bernstein, T.P. Biesiadzinski, E.M. Boulton, B. Boxer, P. Brás, S. Burdin, D. Byram, M.C. Carmona-Benitez, C. Chan, J.E. Cutter, L. de Viveiros, E. Druszkiewicz, A. Fan, S. Fiorucci, R.J. Gaitskell, C. Ghag, M.G.D. Gilchriese, C. Gwilliam, C.R. Hall, S.J. Haselschwardt, S.A. Hertel, D.P. Hogan, M. Horn, D.Q. Huang, C.M. Ignarra, R.G. Jacobsen, O. Jahangir, W. Ji, K. Kamdin, K. Kazkaz, D. Khaitan, E.V. Korolkova, S. Kravitz, V.A. Kudryavtsev, E. Leason, K.T. Lesko, J. Liao, J. Lin, A. Lindote, M.I. Lopes, A. Manalaysay, R.L. Mannino, N. Marangou, D.N. McKinsey, D.-M. Mei, J.A. Morad, A.S.J. Murphy, A. Naylor, C. Nehrkorn, H.N. Nelson, F. Neves, A. Nilima, K.C. Oliver-Mallory, K.J. Palladino, C. Rhyne, Q. Riffard, G.R.C. Rischbieter, P. Rossiter, S. Shaw, T.A. Shutt, C. Silva, M. Solmaz, V.N. Solovov, P. Sorensen, T.J. Sumner, N. Swanson, M. Szydagis, D.J. Taylor, R. Taylor, W.C. Taylor, B.P. Tennyson, P.A. Terman, D.R. Tiedt, W.H. To, L. Tvrznikova, U. Utku, A. Vacheret, A. Vaitkus, V. Velan, R.C. Webb, J.T. White, T.J. Whitis, M.S. Witherell, F.L.H. Wolfs, D. Woodward, X. Xiang, J. Xu, C. Zhang, Nuclear Recoil Calibration at Sub-keV Energies in LUX and Its Impact on Dark Matter Search Sensitivity, Phys. Rev. Lett. 134 (2025) 61002. https://doi.org/10.1103/PhysRevLett.134.061002.

[6] H.S. Lee, G. Adhikari, P. Adhikari, S. Choi, I.S. Hahn, E.J. Jeon, H.W. Joo, W.G. Kang, G.B. Kim, H.J. Kim, H.O. Kim, K.W. Kim, N.Y. Kim, S.K. Kim, Y.D. Kim, Y.H. Kim, J.H. Lee, M.H. Lee, D.S. Leonard, J. Li, S.Y. Oh, S.L. Olsen, H.K. Park, H.S. Park, K.S. Park, J.H. Shim, J.H. So, Pulse-shape discrimination between electron and nuclear recoils in a NaI(Tl) crystal, J. High Energy Phys. 2015 (2015) 93. https://doi.org/10.1007/JHEP08(2015)093.

[7] P. Adhikari, J. Anstey, D.J. Auty, M. Batygov, B. Beltran, C.E. Bina, W. Bonivento, M.G. Boulay, J.F. Bueno, B. Cai, S. Choudhary, B.T. Cleveland, R. Crampton, S. Daugherty, P. Delgobbo, P. Di Stefano, G. Dolganov, L. Doria, F.A. Duncan, M. Dunford, E. Ellingwood, A. Erlandson, S.S. Farahani, N. Fatemighomi, G. Fiorillo, R.J. Ford, D. Gahan, D. Gallacher, S. Garg, P. Giampa, D. Goeldi, P. Gorel, K. Graham, A.L. Hallin, M. Hamstra, S. Haskins, J. Hu, J. Hucker, T. Hugues, A. Ilyasov, B. Jigmeddorj, C.J. Jillings, G. Kaur, F. La Zia, M. Lai, S. Langrock, B. Lehnert, M.K. Yazdi, A. Kemp, N. Levashko, M. Lissia, L. Luzzi, I. Machulin, A. Maru, J. Mason, A.B. Mcdonald, T. Mcelroy, J.B. Mclaughlin, C. Mielnichuk, L. Mirasola, A. Moharana, J. Monroe, A. Murray, C. Ng, M. Olszewski, S. Pal, D. Papi, B. Park, M. Perry, V. Pesudo, T.R. Pollmann, F. Rad, C. Rethmeier, L. Roszkowski, R. Santorelli, S. Seth, V. Shalamova, P. Skensved, T. Smirnova, K. Sobotkiewich, T. Sonley, J. Sosiak, J. Soukup, R. Stainforth, M. Stringer, J. Tang, S. Viel, B. Vyas, M. Walczak, J. Walding, M. Ward, S. Westerdale, R. Wormington, Relative measurement and extrapolation of the scintillation quenching factor of α -particles in liquid argon using DEAP-3600, 123 (2025) 1–9. https://doi.org/10.1140/epjc/s10052-024-13518-7.

[8] L.M. Santiago, H. Bagán, A. Tarancón, G. Rauret, J.F. Garcia, Systematic study of particle quenching in organic scintillators, Nucl. Instruments Methods Phys. Res. Sect. A Accel. Spectrometers, Detect. Assoc. Equip. 698 (2013) 26–36. https://doi.org/10.1016/j.nima.2012.09.041.

[9] M. Pavan, Quenching factor for alpha particles in ZnSe scintillating bolometers, (2017). https://doi.org/10.1088/1742-6596/755/1/011001.

[10] E. V Sysoeva, V.A. Tarasov, O. V Zelenskaya, V.A. Sulyga, The study of α /γ ratio for inorganic scintillation detectors, 414

(1998) 274–278.
[11] B. Zahra, L. Guerbous, H. Bousbia-salah, A. Boukerika, Effect of annealing atmospheres on the scintillation properties of Ce^{3+}-doped YAG nanoscintillator, Radiat. Detect. Technol. Methods 7 (2023) 447–456. https://doi.org/10.1007/s41605-023-00397-x.
[12] B. Zahra, L. Guerbous, H. Bousbia-Salah, A. Boukerika, Effect of Ce^{3+} Content and Annealing Temperature on the Optical and Scintillation Properties of Ce^{3+}-Doped Y3Al5O12 Nanoscintillator Synthesized by Sol–Gel Route, Phys. Status Solidi Appl. Mater. Sci. 220 (2023). https://doi.org/10.1002/pssa.202300022.
[13] M.S.E. Hamroun, A. Guenanou, L. Guerbous, R. Chebout, K. Bachari, Annealing Temperature Effect on Structural and Luminescence Spectroscopy of Y2 SiO5:Ce^{3+} Nanomaterial Synthesized by Sol–Gel Method, J. Res. Updat. Polym. Sci. 11 (2022) 54–60. https://doi.org/10.6000/1929-5995.2022.11.08.
[14] B. Zahra, H. Mekki, L. Guerbous, A. Boukerika, Investigating the influence of pH solution value on the scintillation properties of Ce^{3+}-activated YAG nanopowder synthesized via sol–gel method, J. Radioanal. Nucl. Chem. 333 (2024) 2767–2776. https://doi.org/10.1007/s10967-024-09502-w.
[15] M.J. Kim, H.J. Kim, J.Y. Cho, S. Kaewjaeng, J. Kaewkhao, Crystal growth and scintillation properties of YAG:Ce $^{3+}$ for γ and α detection, Appl. Radiat. Isot. 145 (2019) 126–130. https://doi.org/10.1016/j.apradiso.2018.12.011.